Ultrasonics 105 (2020) 106115

Contents lists available at ScienceDirect

Ultrasonics

journal homepage: www.elsevier.com/locate/ultras

Physical perspective forward-inverse learning for ultrasonic sensing diagnosis in small diameter and thin-wall tube

Xiang Xiao[a], Bin Gao[a,*], Gui Yun Tian[a,b], Zhi Gang Cai[c], Ke qing Wang[d]

[a] School of Automation Engineering, University of Electronic Science and Technology of China, China
[b] School of Electrical and Electronic Engineering, Newcastle University, England, UK
[c] Jiu Li Group Limited by Share Ltd, China
[d] Nanjing University of Information Science & Technology Binjiang College, China

ARTICLE INFO

Keywords:
The thin-wall tube
Ultrasonic inspection
Non-destructive testing

ABSTRACT

The ultrasonic testing method is a well-known non-destructive testing technique which has been applied to the tube inspection for guarantying the quality of the production. However, there exist several challenges to detect the defects of tubes with small diameter and thin-wall due to the complex of multiple reflections and waveform conversion. Parameters selection of the transducer takes key role to enhance the detection sensitivity such as frequency, size, refraction angle, distance offset, and focal point distance. This selection is generally dependent on human experience as it is highly time-consuming and subjective. In this paper, a novel parameter selection method based on physical perspective linked forward-inverse intelligence strategy has been proposed for ultrasonic immersed testing method. The optimized parameters can be calculated automatically while both testing and calibration repeated experiments can be avoided. The proposed method is computationally affordable and yields a high accuracy objective performance. Both simulation and experiments have been conducted to verify the efficacy of the proposed method.

1. Introduction

The small diameter and thin-wall tubes are widely used in nuclear, thermal power, aviation and other industrial fields [1]. These tubes work for a long time in harsh condition such as high temperature, high pressure, nuclear radiation environment, gas liquid two phase scouring or corrosion. During the production process, these tubes undertake defects such as cracks, inclusions, pressing pits, delamination, scratches, etc. These defects are distributed in both inner and outer surface of the tube [2]. When the defect size exceeds the size which is specified in the acceptance standard, the risk of bursting or leakage will increase significantly. Therefore, nondestructive inspection is highly required.

Different techniques are used to inspect cracks for stainless tubes. Bobbin probes based on Eddy Current Testing (ECT) methods have been used for heat exchanger in nuclear power plants [3–4]. Besides, the Motorized Rotating Pancake Coils (MRPCs) are used to examine longitudinal cracks by recording data at scanning points along the tube [5]. However, both coils have difficulties at detecting defects with a particular orientation due to the unsensitive direction between the induced eddy current and the distribution of the defects. The Eddy Current Array [25] (ECA) is a new detection technology which can be applied to detect defects with any orientation. However, there exists a challenge for ECA due to the insufficient detection depth. If the thickness of the tube is more than 2 mm, the ECA is less sensitive for the deep defect conductor due to the skin effect. Besides, the ECA probes with different diameters should be fabricated to suit the different specifications of tubes. Thus, the cost of ECA probes is much higher than that of the conventional ultrasonic probes. The Computed Radiography (CR) has been applied in evaluation the thickness of tube wall [6]. However, compared with other NDT methods, CR has limitation due to the radiation and high cost. Also, the defects in thin-walled tubes are very small and cannot be detected by X-ray due to the sensitivity of x-rays is nominally 2% of the materials thickness [27]. For a tube having the thickness of 8 mm, the smallest defect that could be detected by x-ray would be 0.16 mm. Thus, the smaller defects will not be detected which cannot satisfy the requirement of the nuclear industry. Ultrasonic testing has characteristics of strong directivity, concentrated energy and strong penetrating ability. Zieli Dutra Thomé uses ultrasound to detect defects for fuel rod in Nuclear Pressurized Water Reactor (PWR) [7]. Schwarz developed an ultrasonic array for endoscopic application in medicine and non-destructive testing (NDT) [8]. The ultrasonic phased arrays technology has been applied for leak detection in sodium heated

* Corresponding author.
E-mail address: bin_gao@uestc.edu.cn (B. Gao).

https://doi.org/10.1016/j.ultras.2020.106115
Received 23 September 2019; Received in revised form 24 November 2019; Accepted 24 February 2020
Available online 10 March 2020
0041-624X/

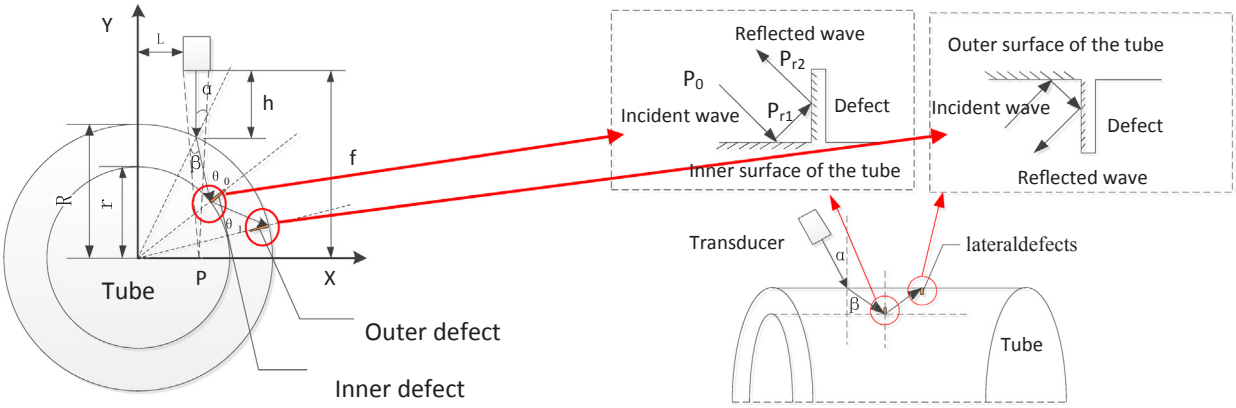

Fig. 1. (a) A schematic diagram of longitudinal defects inspection; (b) a schematic diagram of circumferential defect inspection.

steam generator [24]. A linear phased array UT system for pipe/tube inspection is developed by Guo Y. [22,23]. However, the mechanical rotation scanning is unavoidable in the tube inspection system due to the failure of circumferential and longitudinal electronic scanning. Therefore, the advantage of PA (Phased Array) is not evident. In particular, if the elements are required to cover both the circumferential and the axial directions of the tube, a large number of elements are required. This may lead to out of the maximum number supported by the instrument. Moreover, the ultrasonic phased array system is much more expensive than conventional ultrasound. Taking the economy into consideration, the phased array ultrasonic flexible sheering characteristic is not necessary due to the regular shape of the tube. A rotary unit for flaw detection is developed by Abend [9] and its rotational speed can reach from 0 to 7500 rev/min and the ultrasonic guided wave is applied in testing rock bolts [10].

However, how to correctly select the key parameters of the transducer to reach the optimal performance is highly dependent on manually setting. The results are acceptable, but generally not predictable. In previous research, the parameters of the transducer are illustrated directly whereas the setting problem is ignored. Roh Y, Wang H and Thomas focus on developing, designing and optimizing the performance of ultrasonic transducers [11–13]. However, whether the transducer is suitable for testing a specific specimen is ignored. This is especially for testing tubes with diameter less than 10 mm and wall thickness less than 1 mm. Because of the small diameter and thin wall thickness, the propagation of a sound beam is significantly complicated. Multiple reflections can occur during ultrasonic propagation in the small-diameter and thin-wall tube. These longitudinal and transverse waves are constantly reflecting and interfering while the incident, reflected and scattering beams are complex. The ambiguity waves appear after the multiple reflections. It leads to the computation cost and brings difficulties to distinguish between the defect echo and the ghost signal. In practice, once the frequency and focal length of the transducer are selected, the incident angle and water column should be adjusted to make the echo amplitude of the inner and outer defects as close as possible. According to the tube defect detection standards of ASTM E213-83 and ASTM B118-90, this difference should be as close to or less than 2 dB [15]. However, real experiments illustrated that the echo amplitude of the inner defect is either too high or too low or even no signal. The reason is that one or several parameters of transducer are adjusted incorrect. Thus, this will cause time-consuming to test the inner and outer defects echoes back and forth in the absence of the theoretical guidance. In the traditional method, the selection of parameters for transducer is depending on the human experience by fabricating several transducers with different parameters. The performance of the testing is highly relying on manual selection and this might not be optimized. Although the capability of defect detection can be improved to a certain extent by adding the Time Compensation Gain (TCG) point, the improvement is limited because the noise of the signal is amplified when the gain is increased.

To solve above problems, a novel parameter selection strategy based on physical perspective forward-inverse learning has been proposed for the testing of a thin-wall stainless tube. Both experiments and simulations show that the energy distribution of ultrasound in tube is focused and uniformly distributed. It enables (1) the optimized parameters of transducer can be calculated automatically without additional experiment in advance; (2) It can be robustly applied and expanded to different kinds of tubes.

The rest of the paper is organized as follows: Section 2 discusses the principle of defects detection by using transverse wave. Section 3 describes the selection process of the optimized parameters. Section 4 shows the experimental setup and results. Finally, Section 5 concludes the works.

2. The proposed methodology

2.1. Introduction of ultrasonic measurement of water immersion method

In the process of tube production, there exist longitudinal defects along the axial direction and lateral defects along the circumferential direction. It is difficult to detect defects by applying the direct contact way because of its big curvature. The contact surface of the conventional probes does not fit well with the outer wall of small diameter thin wall tubes, which will greatly affect the accuracy of the measurement. Therefore, ultrasonic water immersion method is applied to detect defects [15]. To interpret the ultrasonic testing of the water immersion, the schematic of the detection system is shown in Fig. 1. The transducer is rotating around the center of the tube to cover 100% detection area. Two sets of transducers [14] should be used to detect the defects distributed along the axial and circumferential directions as shown in Fig. 1(a) and (b), respectively. Fig. 1(a) shows the way to detect longitudinal defects. On the contrary, Fig. 1(b) shows the way to detect lateral defects. Both of longitudinal and lateral defects are detected by using transverse wave.

The principle in transverse wave detection is to put the immersion focusing longitudinal transducer in the water. The generated longitudinal wave will pass through the water column and incident into the tube at a certain angle. When the wave beam reaches the water-steel interface, the refraction and reflection will occur. The refraction longitudinal and transverse waves will be produced inside the tube. To minimize the signal chaos caused by the wave conversion and enhance the detection ability for small defect, the transverse wave is used. Therefore, the incident angle should be adjusted between the first critical angle and the second critical angle. In this situation, the transverse wave is produced without longitudinal waves in tube. The incident angle meets the Eq. (1):

$$\frac{C_{L1}}{C_{L2}} \le sin\alpha \le \frac{r}{R}\frac{C_{L1}}{C_{s2}} \quad (1)$$

where the variable C_{L1} is the propagation velocity of the longitudinal wave in the water and the C_{L2} is the propagation velocity in the steel. The variableC_{s2} is the propagation velocity of the transverse wave in the steel. The r and R represent the inner and outer diameter, respectively. The variable α is an incident angle.

2.2. The proposed physical perspective forward calculation

Many factors that affect defect detection performance. These include frequency, incident angle, transducer diameter and the eccentricity. The mismatch of any parameters will cause the low detection performance. Although the detection signal can be improved by adding TCG point, the improvement is limited. The higher the gain is, the lower the signal-to-noise ratio is. The gain denotes the TCG (Time Compensation Gain). It can adjust the gain of A-scan waveform in segments to conduct distance compensation. The propagation time or distance in the A-scan wave can be divided into segments. Each segment has its gain to amplify the signal. Unlike traditional gain, TCG affects SNR of A-scan signals. It is necessary to find a feasible method to solve these problems.

In the proposed method, the parameters affecting the performance of NDT will be divided into two parts. One part is calculated by physical perspective forward analysis to confirm the parameters of the refraction incident angle, eccentricity and focal length. The second part is that the transducer diameter and frequency automatically obtained by inverse learning of artificial intelligence strategy due to the difficult calculation. Therefore, the proposed architecture of the working procedure can be illustrated in Fig. 2. The first step is building the physical perspective forward model to calculate the parameters and the second step is an iterative testing process which uses ANN-learning (Artificial Neural Network learning) to obtain the optimal parameters by establishing criteria based on acoustic field and digital image processing. After the training is completed, the optimized parameters of transducer will be obtained. As shown in Fig. 2, the optimization of size and frequency is estimated by the inverse learning calculation method and the other parameters can be calculated by physical perspective forward analysis. The optimization process is iterative. It includes three parts: sound-field calculation, evaluation and ANN. The sound-field is used to calculate energy distribution. The evaluation system will give the result of the judgment according to the sound-field. Finally, the ANN conducts machine learning based on the given result by evaluation to conduct the regression.

(1) Calculation of the incident angle

According to Eq. (1) and the structure of water immersion inspection shown in Fig. 1, the incident angle is selected within a certain range. In previous work, the adjustment of the incident angle depends on the experience of the operator.

To calculate the optimized incident angle, we use principle of corner reflection to detect inner and outer defects of the thin-wall tube. When ultrasonic waves pass through the water column into the tube, the incident wave will reflect each of the two planes at the corner of the defect position. In Fig. 1(b), the corner consists of a plane of the defect and a plane of inner as well as the outer surface of the tube. Therefore, the reflected echo of the corner returns to the probe along the incident direction. That is the reason that the defects can be detected. The reflection coefficient u of the corner reflection is the product of the reflection coefficient u_1 and u_2. According to the definition of the reflection coefficients, the variables $u_1 = \frac{P_{r1}}{P_0}$ and $u_2 = \frac{P_{r2}}{P_{r1}}$ are the reflection coefficients of the two end surface of the corner respectively as shown in Fig. 1(b). The total reflection coefficient u can be expressed as:

$$u = \frac{P_{r2}}{P_0} = \frac{P_{r1}}{P_0}\frac{P_{r2}}{P_{r1}} = u_1 u_2 \quad (2)$$

The relationship between the reflection coefficient u of the transverse wave and incident angle α in steel is shown in Fig. 3. It can be seen that the reflection coefficient u reaches 100% when the incident angle is between 30° and 60°. That is, when the incident angle of ultrasonic wave is between 30° and 60°, the ability to detect defects is the best. Thus, the middle value 45°of the range is selected for detecting lateral defects and used with refraction angle as shown in Fig. 1(b). According to the refractive index formula$\frac{sin\alpha}{C_{L1}} = \frac{sin\beta}{C_{s2}}$, the incident angle α can be obtained as:

$$\alpha = arcsin\frac{\sqrt{2}C_{L1}}{2C_{s2}} \quad (3)$$

It is necessary to make both θ_0 and θ_1 at 30°–60° for longitudinal defect detection as shown Fig. 1 (a). In the same way, it is assumed that θ_0 and θ_1 are approximately 45°, namely,

$$\theta_0 + \theta_1 \approx 90 \quad (4)$$

According to the geometric relationship as shown in Fig. 1 (a), Eq. (5) can be obtained.

$$\frac{sin(180 - \theta_0)}{R} = \frac{sin\beta}{r} \quad (5)$$

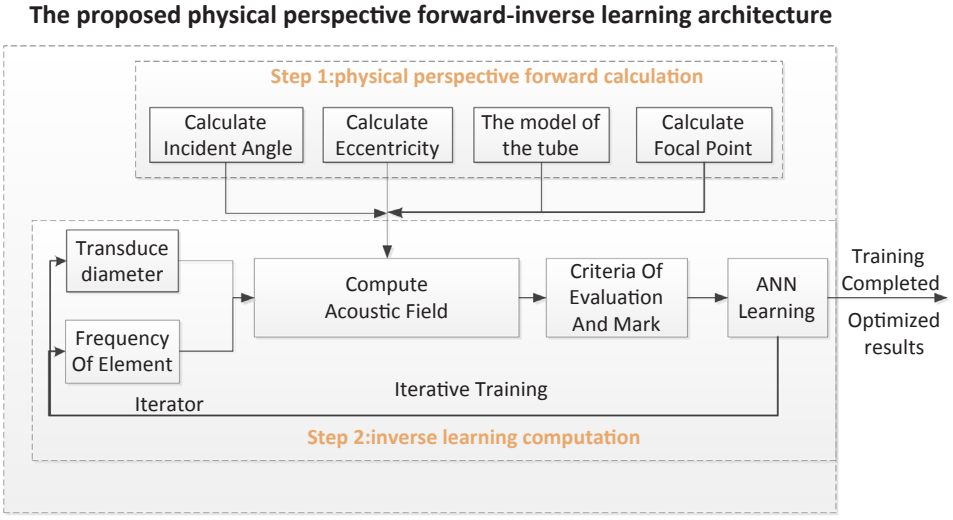

Fig. 2. The schematic of proposed physical perspective forward-inverse learning method.

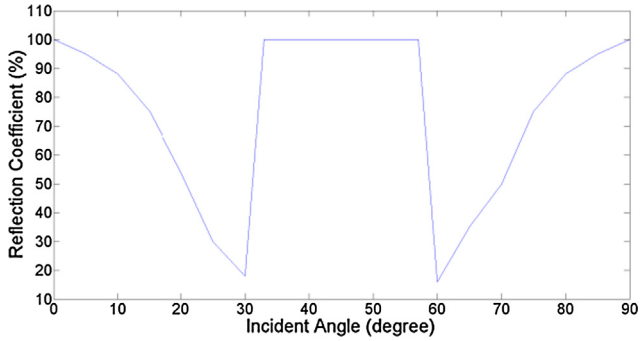

Fig. 3. The relationship of the reflection coefficient for transverse wave.

where the variables R and r represent the outer diameter and inner diameter, respectively. According to the reversibility of the ultrasonic wave propagation process, the angle of refraction from water to steel is equal to the angle of incidence from steel to water after reflection.

$$\beta = \theta_1 \tag{6}$$

After combination of Eqs. (5) and (6), Eq. (7) can be obtained.

$$\frac{sin\theta_1}{sin\theta_0} = \frac{r}{R} \tag{7}$$

Taking Eq. (4) into Eq. (7), Eq. (8) can be obtained.

$$\beta = \theta_1 = arctan(\frac{r}{R}) \tag{8}$$

According to the law of ultrasonic refraction, the ultrasonic incident angle α can be obtained as:

$$\alpha = \arcsin\left\{\frac{C_{L1}}{C_{s2}}\sin[\arctan(r/R)]\right\} \tag{9}$$

Thus, the lateral and longitudinal defects can be detected by using two groups of probes with the incident angle calculated by Eqs. (3) and (9).

It is easy to detect lateral defect as the tilt angle of the probe can be directly adjusted. However, the detection of longitudinal defects is much more complicated. Therefore, the main objective of the proposed method is aiming at the detection of the longitudinal defect.

(2) Calculation of eccentricity

For the detection of longitudinal defects, the incident angle is adjusted by the eccentricity indirectly. According to the structure of the detection, the incident angle is determined by eccentricity. The eccentricity is the horizontal distance between the axis of the probe beam and the central axis of the tube as shown Fig. 1(a). According to the triangle relation, the calculation of the eccentricity is

$$L = Rsin\alpha = \frac{RC_{L1}}{C_{s2}}sin(arctan(r/R)) \tag{10}$$

(3) Calculation of the curvature radius of the acoustic lens

The immersion focal transducer consists of the probe with 0° and acoustic lens. The acoustic lens is used to make the beam focused. In the traditional method, the curvature radius of the acoustic lens will be the R and the focal length will be the F [16]. However, in the immersion inspection method, the medium of ultrasonic wave propagation is not homologous. The ultrasonic wave passes through the water and propagates in the steel. The refraction occurs at the interface between water and steel. In addition to this, ultrasonic wave enter the tube at a certain angle. Therefore, the real focal point p_v will be shorter than the ideal focal point p as shown in Fig. 4. The relationship between the ideal focal length F and the curvature radius of the acoustic lens R can

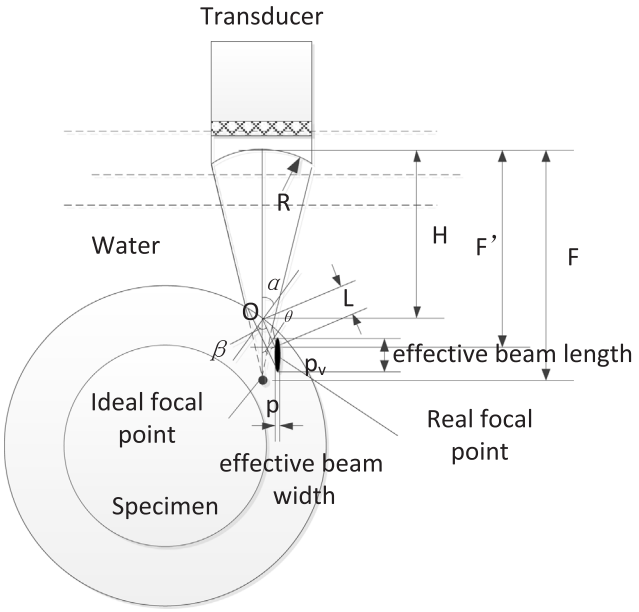

Fig. 4. The model of the immersion focal transducer.

be obtained as:

$$F = \frac{C_1 R}{C_1 - C_2} = \frac{nR}{n-1} \tag{11}$$

where the C_1 and C_2 are the ultrasonic velocity in plexiglass [34] and in water, respectively and the n is a wave velocity ratio$n = c_1/c_2$.

According to the principle of geometrical acoustics, the distance L from the real focal point p_v to the incident point O can be obtained [26] as:

$$L = (F-H)\frac{sin\theta cos(arcsin(m * sin(\alpha - \theta)))}{cos(\alpha - \theta)sin(\beta - arcsin(m * sin(\alpha - \theta)))} \tag{12}$$

where $m = c_3/c_2$ denotes the wave velocity ratio of sound velocity in steel C_3 and sound velocity in water C_2. The θ denotes the semi-diffusion angle and α, β are the incident and refractive angle, respectively. The H is the water column. Thus, the real focal point length F' can be calculated as:

$$F' = cos(\beta - \alpha) * L \tag{13}$$

When the F' is selected, taking Eq. (13) into the Eq. (12), the water column H can be calculated as:

$$H = F - \frac{wF'}{cos(\beta - \alpha)} \tag{14}$$

where $w = \frac{\cos(\alpha-\theta)\sin(\beta-\arcsin(m*\sin(\alpha-\theta)))}{\sin\theta\cos(\arcsin(m*\sin(\alpha-\theta)))}$.

Based on the above equations, the focal point can be produced. In this paper, the ultrasound beams pass through water and then enters the inside of the tube. It is not homogeneous medium. The ultrasound will refract at the interface of water-steel. Since the incident angle is not zero and the beams have a certain width, each beam will not converge to the same location. Not all the beam line has the same incident angle as shown in Fig. 4. Thus, the real focal point will no longer be a point but an ellipse. If the defect located in the area of the focal point, the best testing performance will be obtained.

2.3. The proposed inverse learning calculation

The transducer diameter and frequency are the factors that affect the detection sensitivity and testing performance. Most of the previous works [28–32] have not focused on the optimization in calculation of the size and frequency for the ultrasonic crystal in a small diameter

Table 1
The specific procedure of proposed method.

1. The parameters are calculated by Eqs. (9)–(10) and (13)–(14)
2. Within a certain range of values, set sufficient combinations of frequency and size of the transducer
3. Iteration operation is started. One of the combinations of frequency and size values as the parameters are calculated by step (a) from the simulation of sound field
4. The results of sound field calculation are evaluated by the custom criteria. The judgments of criteria can be divided into three categories of good, middle, bad represented by scores
5. After that all the parameters and judgments of the evaluation custom criteria are used to train the neural network
6. Finally, the neural networks are trained until all combinations of frequencies and sizes are calculated

tubes. The size and frequency of the ultrasonic transducer are given directly by empirical selection. Therefore, the inverse learning calculation based on application of sound field, edge extraction, artificial intelligence strategy based on back-propagation training and established custom criteria are proposed. The back-propagation artificial intelligence strategy is a multi-layer feed-forward network trained according to error back-propagation algorithm and is one of the widely applied neural network models. It can be used to learn and store a great deal of mapping relations of input-output model, and no need to disclose in advance the mathematical equation that describes these mapping relations.

The specific procedure of the proposed method can be summarized as Table.1:

The successful trained neural network will give the detection parameters of the ultrasonic transducer for the unknown tube.

(1) Computation of the sound field

The sound field is computed to find the optimized combination of size and frequency. The sound field computation uses the concept of spatial impulse responses as developed by Tupholme and Stepanishen [17–19]. This response gives an emitted ultrasound field at a specific point in space as a function of time. The field for any kind of excitation can be found by convolving the spatial impulse response with the excitation function.

The purpose of establishing sound field is to analyze the energy distribution of ultrasonic wave based on image processing algorithm. At the same time, the evaluative result is based on the sound field. All parameters including incident angle, eccentricity, the curvature radius of the acoustic lens, water column and ultrasound velocity in water and steel are conducted into the sound field computation. Because the transducer diameter and frequency are not easy to be calculated, the iterative computation method is used to obtain the optimized result. Both frequency and size are selected within a certain range and they can be combined arbitrarily. Best combination is judged by the evaluation system based on the custom criteria as shown in Fig. 2.

(2) The evaluation system based on digital image processing

In the evaluation system, firstly, the edge of sound-field image is extracted. Secondly, the EBW and EBL can be obtained by contour tracking algorithm. Thirdly, the distribution and position relationship of sound-field energy (EBW and EBL) in tube can be judged by logic calculation. At least, the results judged by logic calculation are used to train the ANN. The criteria of evaluating the sound field distribution are the key to the correctness of the proposed ANN learning calculation. This is because the higher the frequency, the shorter the wavelength, the longer the near-field length are bad for ultrasonic testing. In the near-field area, there will be a series of points with maximum and minimum sound pressure due to the wave interference. For any point on the axis of the wave source, the sound pressure P can be expressed as:

$$P = 2P_0 sin\frac{\pi}{\lambda}(\sqrt{\frac{D_s^2}{4} + x^2} - x) \tag{15}$$

where the P_0 is the wave source sound pressure, the D_s is the radius of the wave source and the variable x is the distance from the point on the axis to the wave source.

According to Eq. (15), when the sound pressure P reaches the maximum, then $sin\frac{\pi}{\lambda}\left(\sqrt{\frac{D_s^2}{4} + x^2} - x\right) = \sin(2n+1)\frac{\pi}{2} = 1$, the following formula can be obtained as:

$$x = \frac{D_s^2 - \lambda^2(2n+1)^2}{4\lambda(2n+1)} \tag{16}$$

According to Eq. (15), when the sound pressure P reaches the minimum, then $sin\frac{\pi}{\lambda}\left(\sqrt{\frac{D_s^2}{4} + x^2} - x\right) = sin(n\pi) = 0$, the following formula can be obtained as:

$$x = \frac{D_s^2 - (2n\lambda)^2}{8n\lambda} \tag{17}$$

where $n = 0, 1, 2, 3, \cdots, (D_s - \lambda)/2\lambda$, λ is wavelength. As Eqs. (16) and (17) shown, a series of points with maximum and minimum sound pressure exist. The echoes of big defects at the minimum of sound pressure might be low whereas the echoes of small defects at the maximum of the sound pressure might be high. This will lead to misjudgment or failure detection. At the same time, the frequency is too high, the SNR (signal to noise ratio) decrease significantly. On the contrary, according to$\theta_0 = 70\lambda/D_s$, where the variables θ_0 and λ are semi-diffusion angle and wavelength, respectively. It indicates that the higher the frequency is, the smaller the semi-diffusion angle is, the better the directivity of the beam is, therefore, the energy is concentrated. Thus, this is helpful to distinguish the defects on the outer and inner surface of the tube. According to the conservation of energy, the energy distributed inside the tube should be equal to the energy of the wave source without considering attenuation. Therefore, the more dispersed the energy, the lower the sound pressure and the lower the defect echo amplitude. Moreover, the larger the transducer size, the better the beam directivity and the more concentrated energy, which is helpful to improving the sensitivity of the flaw detection. Nevertheless, due to the waveform transformation at the interface between the water and steel, the larger the size is, the more longitudinal waves will be produced, which will affect the defect detection.

Therefore, to solve this problem, both size and frequency should be taking into comprehensive consideration. The criteria of evaluation are established based on the concept of EBW (effective beam width) and EBL (effective beam length) as shown in Fig. 4. In the criteria, the EBW of the transducer does not exceed 0.5 mm. The ratio of the length of the standard defect to the EBL of the transducer should be between 0.3 and 1. The ratio of the probe focal length F to the crystal element diameter should be within the range of 1.8–5. The main beam should cover the entire wall of the tube and obtain more concentration.

To obtain the value of EBW and EBL as well as the distribution of energy, we use the edge extraction by applying a contour tracking algorithm [20]. The pixels of the image are convolved with a Laplacian-of-Gaussian (LoG)operator and the edges are detected at the zero-crossing points[33]. Thus, the value of EBW and EBL can be obtained by the proportional relationship between pixels and dimensions [20].

(3) The back-propagation artificial intelligence strategy

The artificial intelligence strategy is applied for solving the inverse problems with complex internal mechanisms. Each group of input values will be evaluated as good, middle or bad judgment represented by scores. The training is completed by inputting the samples which are composed of the results of the evaluation system and the combinations

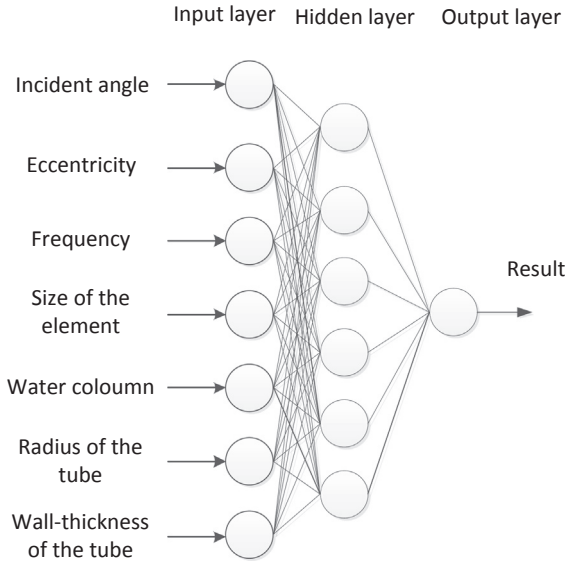

Fig. 5. The structure of artificial intelligence strategy.

with different parameters until the error between the output value target and the output value of the target does not decrease. The structure and the input parameters of the network are shown in Fig. 5. It conducts tutorial learning based on the given result by evaluation to conduct the regression. There are seven neurons in the input layer and the parameters are incident angle, eccentricity, transducer diameter, water column, radius and thickness of the tube. There are six neurons in the hidden layer. The output layer is one neuron which is a variable. The incidence angle, eccentricity, water column can be obtained by physical perspective forward calculation. Therefore, the other training data of frequency and transducer diameter are divided into several combinations. There are eight frequencies: 2 MHz, 4 MHz, 6 MHz, 8 MHz, 10 MHz, 12 MHz, 14 MHz and 15 MHz. The training data of transducer diameter are Φ6, Φ8, Φ10, Φ12, Φ14, Φ16. Therefore, for one kind of tube, there are 48 combinations in training data. Besides, the training data of the tube are divided into several combinations. There are six tube diameters in the training data; it ranges from 6 mm to 16 mm with 2 mm intervals. The thickness of the tube are 0.5 mm, 0.7 mm, 0.9 mm, 1 mm, 1.2 mm, respectively in the training data. In general, the total number of training data is 1440 ($6 \times 5 \times 48$). During the training process, the weight decay is used to prevent overfitting problem. It is equivalent to norm regularization. By adding penalty terms, regularization makes the learning model parameters smaller. We can train regression models with different λ to have a good inhibition on overfitting. The purpose of the proposed regression task is to find out the relationship between ultrasonic parameters and evaluated scores calculated by evaluation system. The group of ultrasonic parameters with high scores is the expecting results of the optimization. Once the network training is completed, the regression model is established. Through this regression model, we can find out the optimized frequency and transducer diameter for the testing tube.

3. Simulations and experiments setup

To validate the proposed technique, taking a tube with a diameter of 6 mm and a wall thickness of 0.677 mm as an example, the simulation and experiment are carried out. The other samples of Φ10 × 0.7 mm and Φ14 × 1 mm are tested as well. The specimen is made by the manufacturers of zirconium alloy cladding tubes which are used for the nuclear power plant. The material of the tube is zirconium alloy. In the specimen, there are two defects located in the inner and outer surface of

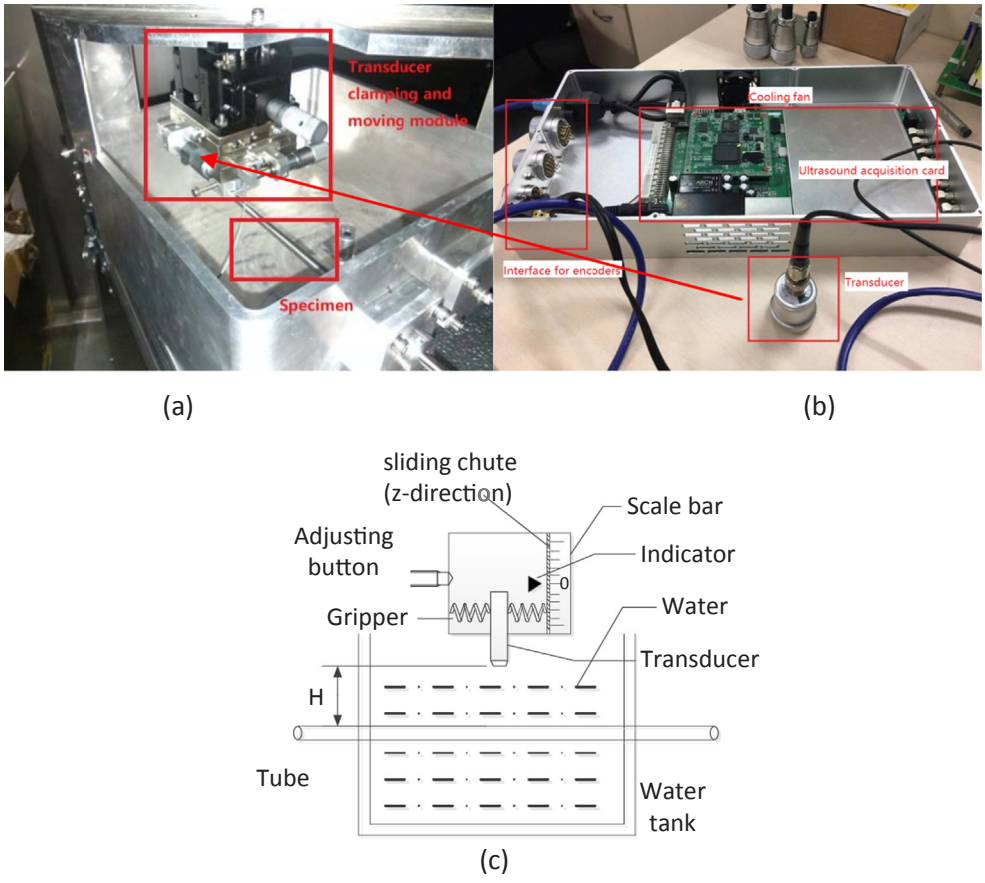

Fig. 6. (a) The device and specimen for testing; (b) the acquisition system; (c) the schematic of the device.

Table 2
The result of proposed method.

Incident angle	Eccentricity	Focal length	Size	Frequency
26.1°	1.2 mm	30 mm	Φ14	15 MHz

the tube, respectively. The size of inner/outer defect is 2 mm (length) × 0.5 mm (width) × 0.05 mm (depth) as shown Fig. 1 (a). The model of specimen and defects is established in simulation. The simulation is calculated by using CIVA software in which developed by CEA (French Atomic Energy Commission). At the same time, mechanical devices and transducers with different parameters are fabricated for testing as shown in Fig. 6(a). With the device, the transducer can be moved along *x-y-z* directions arbitrarily with calibration. When the indicator is located at the zero point, the distance H between the transducer to the tube can be measured by using ruler or vernier caliper. The z-direction shift Δz can be adjusted by adjusting the button and read out from the scale directly. Then the distance from the transducer to the tube can be obtained by calculating$z = H + \Delta z$ as shown in Fig. 6 (c). The measuring principle of shifting along the x and y directions is the same as that of the z axis. The frequency from 2 MHz ~ 15 MHz and size from Φ8 mm ~ 14 mm of the transducers are simulated and tested. The parameters of the transducer are shown in Table 2 and 3, respectively. Fig. 6(b) shows the ultrasound acquisition system. The acquisition card can detect four channels at the same time with working frequency from 0.2 MHz to 20 MHz. The acquisition card is made by university of electronic science and technology with four ultrasound channels. The transducers are made by Guangzhou Doppler Electronic Technologies Co., Ltd. During the sampling process, the gain can be adjusted from 0 dB to 80 dB and the Repetition Pulse Frequency (RPF) is set as 2 KHz.

In order to validate an accuracy of the inspection with variations in defects, the Φ6 × 0.677 testing tube with 0.05 mm, 0.15 mm, 0.25 mm,0.35 mm (depth) inner and outer defects detection are also involved in the revised paper. All of these defects are 2 mm length and 0.5 mm width. Each type of inner defects and outer defects are located at the same position along the axial direction. The space between the defects is 2 mm along the axial direction as shown in Fig. 7(a). The inner defects and outer defects distributed at 0°and 90° along the circumferential direction respectively as shown in Fig. 7(b).

4. Experimental results and discussion

For the experimental specimen, the parameters are given by the proposed method as shown in Table 2. According to the Table 2, the sound field of the transducer, simulation of defects response, the result of image edge extraction and the distribution of the ultrasonic energy in tube are carried out as shown in Fig. 8. The color of Fig. 8(a) and (d) represents for the ultrasound energy value. It can be seen that the focus area is exactly concentrated in the target region and the entire wall of the tube is covered completely as shown in Fig. 8(a) and (d), respectively. Fig. 8(b) is the focal area extracted from the result of the sound field by using contour tracking algorithm. The effective beam is encapsulated completely and correctly. The EBW and EBL are measured by using digital image processing of 0.26 mm and 3.45 mm, respectively. This is validated with the established experiential criteria and standards [21]. Fig. 8(c) is the simulation scanning image of defects on the inner and outer surfaces of the tube. It can be seen that the energy of ultrasonic wave focused well within the tube. The signal of the second-reflected wave is clear without clutters. Both defects can be detected easily and there is no ghost wave affecting the judgment.

The simulation of different transducers has been carried out. The defects response of the transducer with a crystal element size from 8 mm to 14 mm at 15 MHz frequency is shown in Fig. 9. Fig. 9(a) and (b) show the inner and outer defects by using A-scan respectively. It can be seen that the response signal of defects increases with the increase of crystal element size due to the increased energy. However, the transducer diameter should not be too big because sound beam's incident angle will be less than the first critical angle due to the circular tube. Then the longitude wave will exist in the propagation in which affecting the analysis of defect. The scanning of the transducer with frequency from 2 MHz to 10 MHz is simulated as shown in Fig. 10. Compared with 15 MHz frequency transducer, the signal of different transducers has a lot of clutters that affecting the defect judgment. These are shown in Fig. 10(a) and Fig. 10(b) where the SNR is low. The transducer with low frequency has lower timing resolution. In Fig. 10(a), the inner and outer defects cannot be distinguished by ultrasonic flight time. This is because the energy concentration of the transducer varies with the frequency. Fig. 8(c) shows that the transducer energy of the 15 MHz frequency is the most concentrated. It can be seen that after the wave reflecting at the inner surface of the tube, there are clutters made by the wave transformation. The Fig. 11 is an analysis of the sound field. In Fig. 11(a), the energy of sound field is not concentrated, and it is distributed in the whole medium. According to the conservation of the energy, the energy distributed inside the tube should be equal to those of the wave source without considering attenuation. Therefore, the more dispersed the energy, the lower the sound pressure as well as the lower the defect echo amplitude. The 5 MHz transducer is better whereas it is still not an ideal one as shown in Fig. 11(b). As can be seen

Table 3
The result of other samples by using proposed method.

	No. 1 specimen	No. 2 specimen	No. 3 specimen
Dimension	Φ10 × 0.7 mm	Φ6 × 0.67 mm	Φ14 × 1 mm
Parameters by experience	Frequency:15 MHz	Frequency:10 MHz	Frequency:15 MHz
	Size:φ8 mm	Size:φ14 mm	Size:φ14 mm
	Focal length:25 mm	Focal length:30 mm	Focal length:24 mm
	Water Column:25 mm	Water Column:30 mm	Water Column:24 mm
	Eccentricity:2.33 mm	Eccentricity:1.32 mm	Eccentricity:3.1 mm
Parameters by proposed method	Frequency:15 MHz	Frequency:15 MHz	Frequency:15 MHz
	Size:φ10 mm	Size:φ14 mm	Size:φ14 mm
	Focal length:24 mm	Focal length:30 mm	Focal length:25 mm
	Water Column:24 mm	Water Column:28 mm	Water Column:24 mm
	Eccentricity:2.14 mm	Eccentricity:1.2 mm	Eccentricity:2.9 mm
Amplitude by experience	Inner defect:54.9%	Inner defect:36.9%	Inner defect:36.5%
	Outer defect:15%	Outer defect:25.7%	Outer defect:54.3%
Amplitude by proposed method	Inner defect:69.9%	Inner defect:52.5%	Inner defect:86%
	Outer defect:63%	Outer defect:45.5%	Outer defect:74.3%
Saving time	1–3 day	1–3 day	1–3 day
SNR improved (dB)	Inner defect:2.1 dB	Inner defect:3.1 dB	Inner defect:7.4 dB
	Outer defect:12.4 dB	Outer defect:4.9 dB	Outer defect:2.7 dB

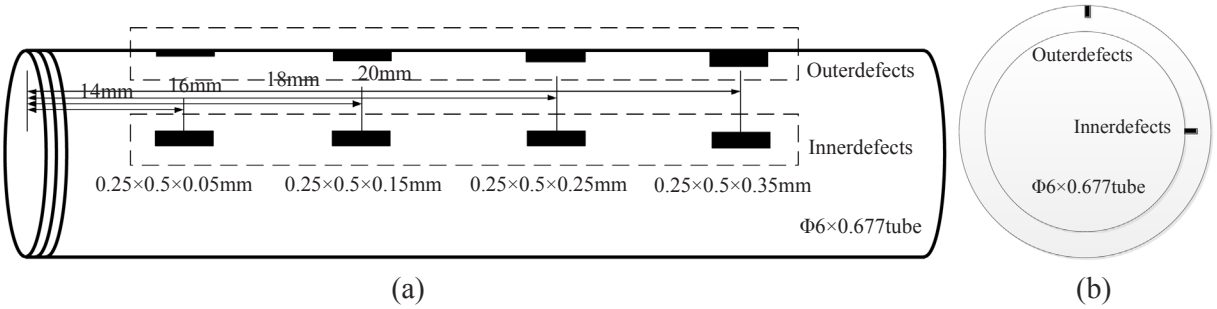

Fig. 7. (a) the distribution of defects along the axial direction; (b) the distribution of defects along the circumferential direction.

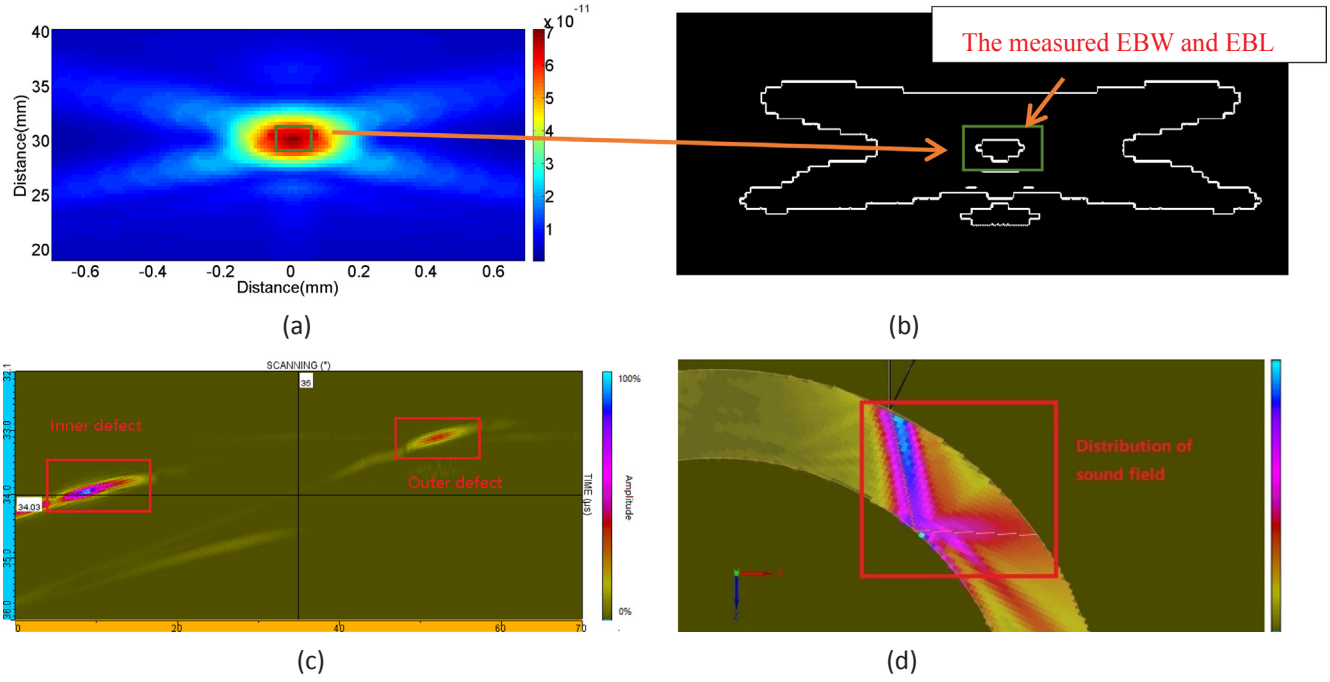

Fig. 8. (a) The sound field of the transducer; (b) the result of image edge extraction; (c) simulation of defects response; (d) the distribution of the ultrasonic energy in tube.

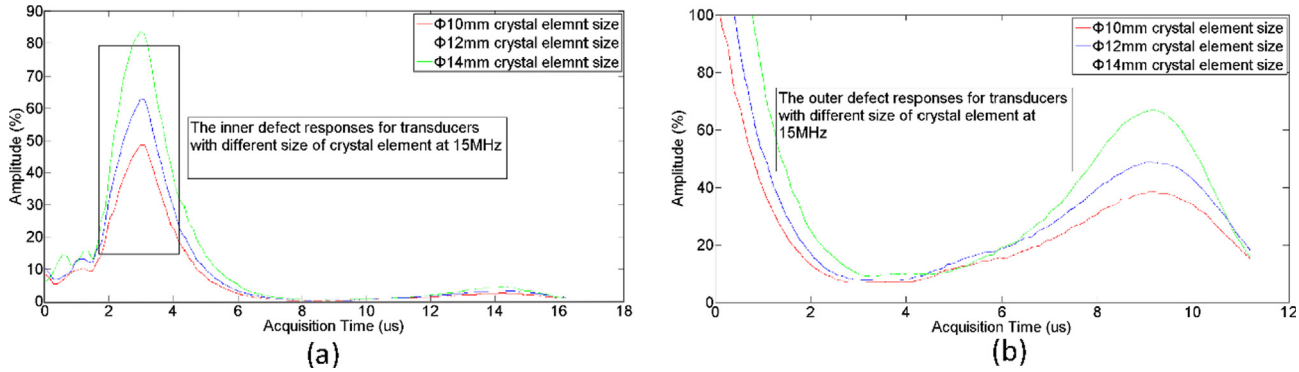

Fig. 9. (a) The inner defect response for transducers with different crystal element size; (b) the outer defect response for transducers with different crystal element size.

from the signals of Fig. 10(a) and (b) corresponding to the sound field Fig. 11(a) and (b), the defects are covered by these clutters, respectively. It will take some time to convert the signal into tomography. The consuming time of imaging region reconstruction depends on the spatial resolution and performance of CPU. The higher the spatial resolution, the longer the time consumed. In this paper, the spatial resolution is set as 0.2 mm and the CPU is Intel I5 with 2.3 GHz. It will take approximately 15 min to construct the image as shown in Figs. 8, 10, 11.

The signal experiment has been carried out as shown in Fig. 12,13. Fig. 12(a) shows the signal response of inner and outer defects by using the transducer with parameters calculated by using the proposed method. In Fig. 12, the A-scan signal with no defect is shown with the green curve and the signal response of the defects is shown with blue

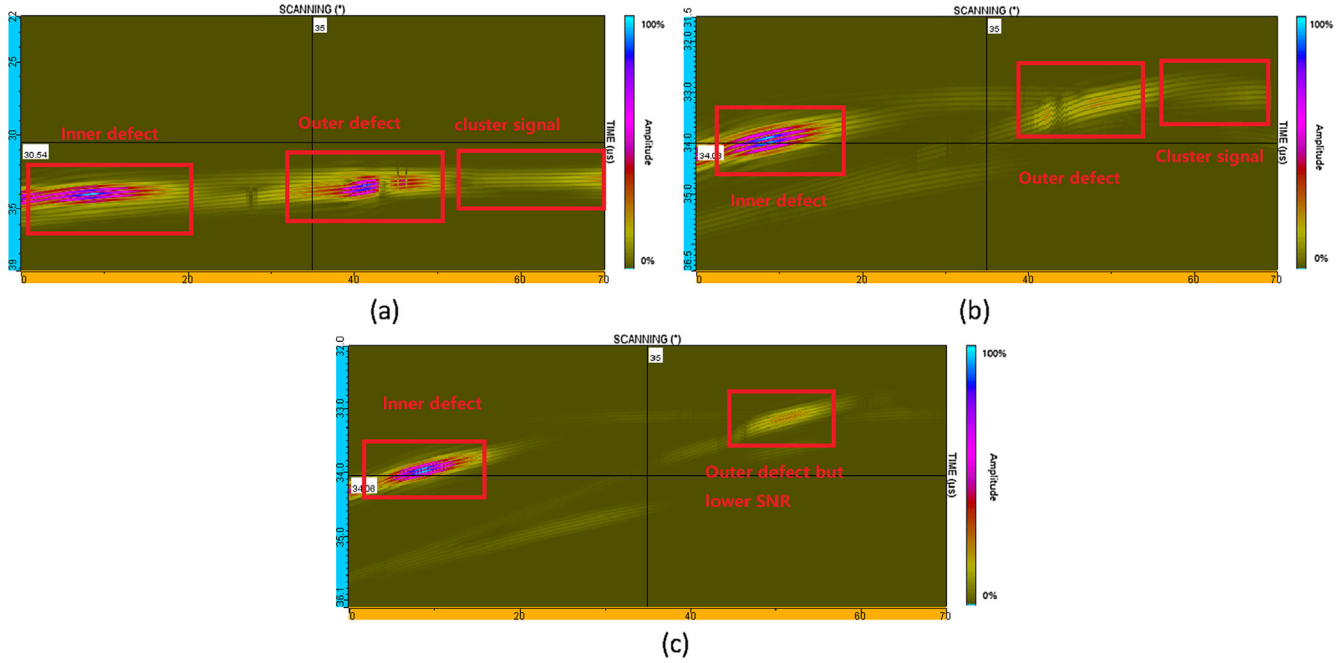

Fig. 10. (a) The simulative scanning for transducer with 2 MHz; (b) the simulative scanning for transducer with 5 MHz; (c) the simulative scanning for transducer with 10 MHz.

and red curve, respectively. The echoes are 52.5% and 45.5% respectively and the difference in the amplitude of inner and outer defects are 7% less than 2 dB which it is no need to do TCG points. It also meets with defect detection standard ASTM E213-83 and ASTM B118-90 in the United States. Fig. 12(b) shows the result of the signal response by using 10 MHz frequency. Though, it meets the requirement, the amplitude of the signal is much lower. If the echo of interface reaches 80% line as Fig. 12(a), the gain should be increased about 6 dB. In this situation, the noise is amplified and the SNR decreased. The other transducers with different parameters are tested as well. The result of defect response by using 2 MHz and 5 MHz frequency are shown in Fig. 13(a) and (b), respectively. It is not suitable by using the lower frequency transducer to inspect small-diameter and thin-wall tube.

Table 3 shows the summary results. It shows that the testing performance from transducer with the parameters selected by the experience is uncertain. The manual parameter selection is a time-consuming process and depends on human experience. It will take 1–3 days to finish the testing work. The process of manual parameter adjustment has several steps.

1. The frequency and size of the transducer are selected manually. These parameters may not suitable for testing the different type of the tube.
2. The response signal amplitude of inner defect is tested by adjusting the incident angle, eccentricity, focal distance and so on. Any one of them will affect the response signal amplitude. Therefore, the adjustment will take long time to judge there are no false defects signals and the echo amplitude should reach 80%.
3. As same as step 2, the response signal amplitude of outer defect is tested by adjusting the incident angle, eccentricity, focal distance and so on.
4. Go back to step 2 to check whether the difference of the amplitude between inner defect and outer defect is less than 2 dB to meet up with the ASTM E213-83 standard. Therefore, the NDT operator will test repeatedly between step2 to step4 due to the response signals of inner defect and outer defect are both affected by the same adjustment. This procedure will consume a long time.
5. If it meets up with the standard, these parameters will be settled. However, if it does not work by step2 ~ step4, then the frequency and size of transducer will be adjusted. This may lead to fabricate a new transducer. After that the above testing steps will be carried out again. Compared with the manual parameter adjustment method, it avoids taking a long time to select the proper parameters of the transducer without prior knowledge for testing one kind of tube.

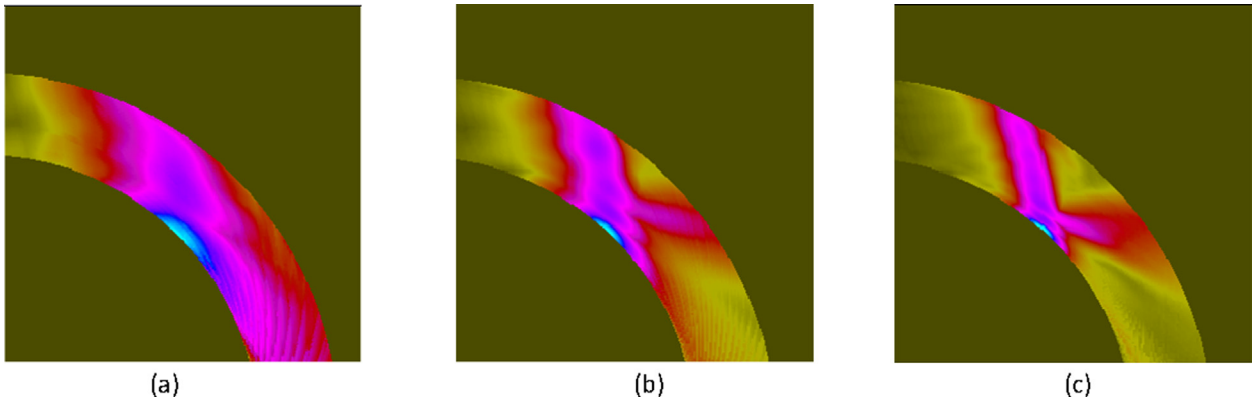

Fig. 11. (a) The sound field of transducer with 2 MHz; (b) the sound field of transducer with 5 MHz; (c) the sound field of transducer with 10 MHz.

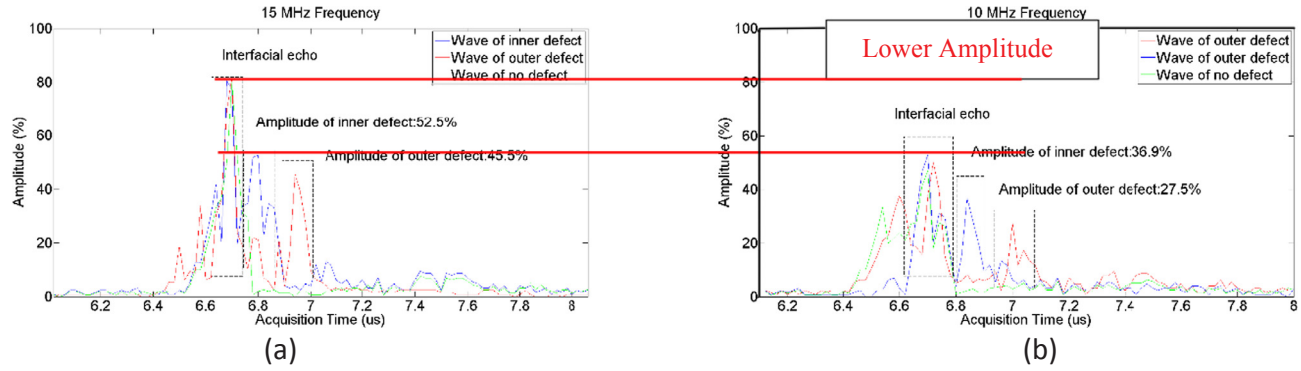

Fig. 12. (a) The defects response at 15 MHz frequency; (b) the defects response at 10 MHz frequency.

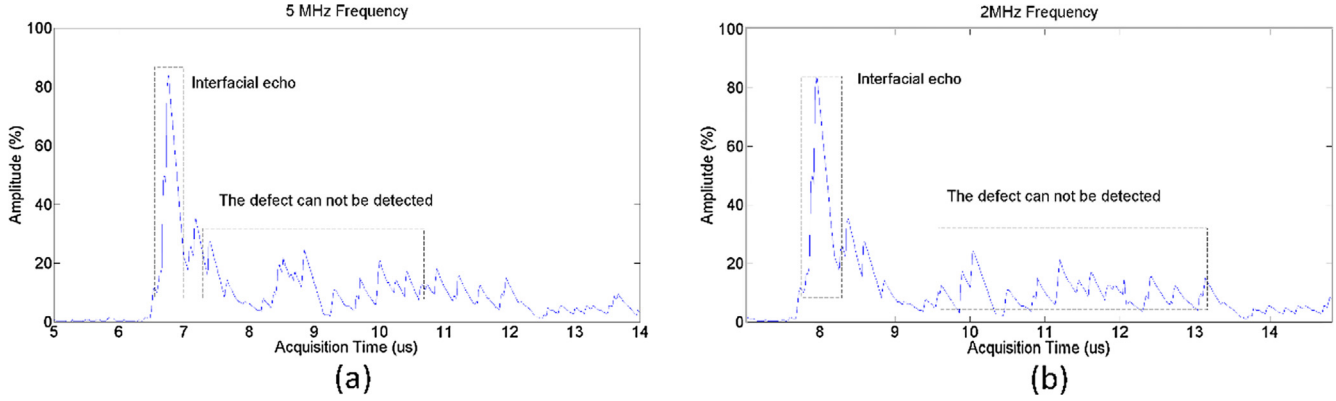

Fig. 13. (a) The defects response at 5 MHz frequency; (b) the defects response at 2 MHz frequency.

Besides, the testing performance is optimized by using the proposed method. The different amplitude of inner and outer defect is within 2 dB for better consistency. In comparison, both time-consuming and echoes gain contrast are applied for validation. Moreover, in the traditional methods, 10 MHz transducer is generally to be selected which lead to the insufficient testing of the transducers with different parameters. The echoes gain contrast of defect detection can be calculated by using signal-to-noise ratio (SNR)$G = 20 * \lg\frac{V_1}{V_2}$, where the variable G is the signal gain, the variables V_1 and V_2 represent the defect signals amplitude of the proposed method and the traditional method, respectively. Therefore, the gain contrast results are shown in Table 3. The testing signal amplitude is improved significantly.

Moreover, the response time is important for automatic inspection. To conduct a real-time imaging, the response time is expected as short as possible. The response time can be divided into two parts when the raw data is received. Firstly, signal filtering is processed by applying FFT. Secondly, Time Compensation Gain (TCG) is conducted. It is the gain compensation for the echoes with different depths along the depth direction. Finally, whole A-scan data are processed to construct a tomography. The proposed method is helpful to shorten the response time. This is because of that it avoids TCG calculation in which caused by manual parameters selection.

The inspection result of defects with different depth is shown in Fig. 14 by using the proposed method. The inner and outer defects relationship between amplitude and defect depth are drawn with blue and red curve, respectively. It can be seen that the defect depth and echo response amplitude are approximately linear correlated. In particular, the trend slows down after the depth which is more than 0.35 mm. This is because the amplitude is related to the reflected energy, when the depth achieves 0.25 mm, most of energy is already reflected back.

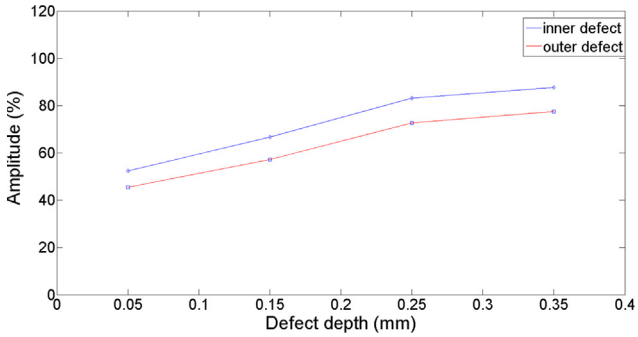

Fig. 14. The relationship between amplitude and defect depth.

The experiment of the position measurement has been carried out by using the transducer selected by the proposed method. The axial positions of the defects are measured as 14 mm, 16.1 mm, 18 mm and 20.1 mm, respectively. The position measurement method is based on −6dB length measurement. Firstly, it is moving the transducer by using the device to find the highest amplitude. Secondly, both end positions where the amplitude drops to half of the highest point are recorded. Then, the defect position is equivalent to the center position and it can be calculated. The measured positions are corrected as the ground truth according to the result.

5. Conclusion and Future work

In this paper, a physical perspective forward-inverse learning method has been proposed to optimize the ultrasonic NDT. It provides theoretical guidance for acoustic parameter selection of automatic inspection for small-diameter and thin-wall tubes. The digital image process and artificial intelligence strategy are applied for automatic

parameter selection. The measurement of the ultrasonic beam and the judgment of the parameters can be given by applying digital image process. These judgments are then used to train the ANN model to confirm an optimized result for parameter selection. Also, a deep analysis regards to the relationship between parameters of the transducer with testing performance has been presented. Both of simulation and experiment results demonstrate that the echoes of the inner and outer defects are meeting up with the ASTM E213-83 standard for thin-wall stainless tube with 6 mm diameter and 0.677 mm wall thickness. Several conclusions can be drawn: (i). this method avoided the wave cross-talk caused by the big curvature of the tube; (ii). the proposed method enables us the optimized parameters of transducer can be calculated automatically without any real transducer signal test and testing experience ahead; (iii). It can be robustly applied and expanded to different kinds of tubes. Future work will carry out the detection with ultrasonic transducer array to improve the scanning velocity.

Declaration of Competing Interest

We declare that we do not have any commercial or associative interest that represents a conflict of interest in connection with the work submitted.

Acknowledgments

The work was supported by state administration of quality supervision, inspection and quarantine (No. 2017QK042), supported by National Natural Science Foundation of China (No. 61527803), supported by Science and Technology Department of Sichuan, China (Grant No. 2018GZ0047 and Grant No. 2018JY0655).

References

[1] Pengfei Zhang, Xiufen Zhao, Ying Yin, Guofu Yin, Some studies on ultrasonic defect inspection for small diameter thin-walled steel tubes, FENDT 2013 – Proceedings of 2013 Far East Forum on Nondestructive Evaluation/Testing: New Technology and Application, 2013, pp. 159–165.
[2] D.G. Park, K.S. Ryu, D. Son, Detection of magnetic phase in the steam generator tubes of NPP, InTech (2011) 165–184.
[3] H.M. Sadek, NDE technologies for the examination of heat exchangers and boiler tubes—principles, advantages and limitations, Insight 48 (3) (2006) 181–183.
[4] V. Uchanin, V. Najda, The development of eddy current technique for WWER steam generators inspection, InTech 2011, 2011, pp. 145–164.
[5] Minhhuy Le, Hoanghai Vu, Jungmin Kim, Chandra Sekhar Angani, Jinyi Lee, Quantitative evaluation of corrosion in a thin small-bore piping system using bobbin-type magnetic camera, J. Nondestruct. Eval. 33 (1) (2014) 74–81.
[6] Marko Rakvin, Damir Markučič, Boris Hižman, Evaluation of pipe wall thickness based on contrast measurement using computed radiography (CR), Procedia Eng. 69 (2014) 1216–1224, https://doi.org/10.1016/j.proeng.2014.03.112.
[7] Zieli Dutra Thome, Wagner Coelho Albuquerque Pereira, João Carlos Machado, José Manoel Seixas, William Soares-Filho, A system for nuclear fuel inspection based on Ultrasonic Pulse-Echo Technique, IEEE Trans. Nucl. Sci. 58 (5) (2011) 2452–2458, https://doi.org/10.1109/TNS.2011.2164557.
[8] H.P. Schwarz, H.J. Welsch, P. Becker, M. Biebinger, R.M. Schmitt, Development of a new ultrasonic circular array for endoscopic application in medicine and NDT, Ultrasonics Symposium Proceedings, 1988, pp. 639–642.
[9] K. Abend, O. Slickers, W. Sternberg, Rotating Ultrasonic Transducers for Defect Detection and Dimension Measurement of Tubes, IEEE,, 1974, pp. 688–690.
[10] M.D. Beard, M.J.S. Lowe, Non-destructive testing of rock bolts using guided ultrasonic waves, Int. J. Rock Mech. Min. Sci. 40 (4) (2003) 527–536.
[11] Y. Roh, M.S. Afzal, Optimal design of a sparse planar array transducer for underwater vehicles by inclusion of crosstalk effect, Japanese J. Appl. Phys. 57 (7S1) (2018) 07LG02.
[12] H. Wang, X. Wang, C. He, et al., Investigation and analysis of the influence of excitation signal on radiation characteristics of capacitive micromachined ultrasonic transducer, Microsyst. Technol. 24 (7) (2018) 2999–3018.
[13] G. Thomas, J.Y. Chapelon, J.C. Bera, et al., Parametric shape optimization of lens-focused piezoelectric ultrasound transducers, IEEE Trans. Ultrasonics Ferroelectrics Freq. Control PP (99) (2018) 1–1.
[14] X. Xiao, B. Gao, G.Y. Tian, et al., Novel ultrasound system with intelligent compensate sensing for high precision measurement of thin wall tube, IEEE Sens. J. PP (99) (2018) 1-1.
[15] R.B. Thompson, D.O. Thompson, Ultrasonic in nondestructive evaluation, Proc. IEEE 73 (12) (1985) 1716–1755.
[16] S. Chen, A. Sabato, C. Niezrecki, et al., Characterization and modeling of the acoustic field generated by a curved ultrasound transducer for non-contact structural excitation, J. Sound Vibrat. 432 (2018) 33–49.
[17] G.E. Tupholme, Generation of acoustic pulses by baffled plane pistons, Mathematika 16 (1969) 209–224.
[18] P.R. Stepanishen, The time-dependent force and radiation impedance on a piston in a rigid infinite planar baffle, J. Acoust. Soc. Am. 49 (1971) 841–849.
[19] P.R. Stepanishen, Transient radiation from pistons in an infinite planar baffle, J. Acoust. Soc. Am. 49 (1971) 1629–1638.
[20] H. Li, B.S. Manjunath, S.K. Mitra, A Contour-based Approach to Multisensor Image Registration, IEEE Press, 1995.
[21] J.W. Xia, C. Han, Ultrasound inspection of zirconium alloy cladding tube for nuclear fuel, Nucl. Power Eng. 3 (2016) 122–126.
[22] Q. Yuan, Y. Guo, Z. Sun, et al., Development of an ultrasonic phased array for nondestructive testing of pipes: theory and practice, Mater. Eval. 69 (4) (2011) 501–506.
[23] Y. Guo, Q. Yuan, Z. Sun, et al., Development of ultrasonic phased array systems for applications in tube and pipe inspection, Aip Conference, American Institute of Physics, 2012.
[24] Y. Chikazawa, T. Yoshiuji, Water experiment on phased array acoustic leak detection system for sodium-heated steam generator, Nucl. Eng. Des. 289 (2015) 1–7.
[25] M.A. Machado, L. Rosado, N. Pedrosa, et al., Novel eddy current probes for pipes: Application in austenitic round-in-square profiles of ITER, NDT E Int. 87 (2017) 111–118.
[26] W. Jun, G. Tie, et al., Analysis and experiments of oblique incident sound field of water-immersed focusing probe, J. Jiamusi Univ. (Natural Science Edition) 23 (3) (2005) 358–361.
[27] S.K. Dwivedi, M. Vishwakarma, A. Soni, Advances and researches on non destructive testing: a review, Mater. Today: Proc. 5 (2) (2018) 3690–3698.
[28] Z.D. Thome, W.C.A. Pereira, J.C. Machado, et al., A system for nuclear fuel inspection based on Ultrasonic Pulse-Echo Technique, IEEE Trans. Nucl. Sci. 58 (5) (2011) 2452–2458.
[29] U. Amjad, S.K. Yadav, C.M. Dao, et al., Advanced signal processing technique for damage detection in steel tubes, Health Monitoring of Structural and Biological Systems 2016, International Society for Optics and Photonics, 2016.
[30] W. Dong, Z. Wu, X. Zhou, et al., Experimental studies on void detection in concrete-filled steel tubes using ultrasound, Construct. Build. Mater. 128 (2016) 154–162.
[31] M.W. Urban, I.Z. Nenadic, C. Pislaru, et al., Measurement of longitudinal and circumferential waves in tubes and artery excited with ultrasound radiation force, 2013 IEEE International Ultrasonics Symposium (IUS), IEEE, 2013, pp. 1765–1768.
[32] F. Dupont-Marillia, M. Jahazi, S. Lafrenier, et al., Design and optimisation of a phased array transducer for ultrasonic inspection of large forged steel ingots, NDT E Int. (2019).
[33] W. Pratt, Digital Image Processing, Wiley, New York, 1991.
[34] K.M. Smyth, Piezoelectric micro-machined ultrasonic transducers for medical imaging, Massachusetts Instit. Technol. (2017).